

# Summary

## Introduction

Rapid environmental change, IPCC, estimated temperature rise.

Trend to precocity in plants, flowering time, etc. Advance in phenology.

**Problem:** Understanding (and predicting?) long-lived plant adaptation to climate change

Based on previously developed demographic and quantitative genetics model (see ), added fluctuating environments. Made theoretical predictions. Estimated fluctuations using data from phenological data (PHENOFIT).

## Materials and Methods

### Population model

We used a previously developed model with stage-structure (Sandell 2014, master's thesis). We considered a population of trees split in two classes, immature (I) and mature (M). only mature individuals reproduce. Each year, an immature individual can survive with a probability  $s_I$ , mature and reproduce with a probability of  $m$ . At the same time, a mature individual has a probability  $s_M$  to survive. First-time reproducers, i.e. immature that became mature and reproduce the same year, have a fecundity of  $f_1$ , while experienced reproducers, those who already reproduced at least once, have a fecundity of  $f_2$ . Produced seeds have a probability  $s_0$  to survive and join the pool of immature trees. The standard parameters set is given in (Table 1). The population census is just before reproduction. The population dynamics can be predicted using the following matrix (Caswell, 2001):

$$A = \begin{pmatrix} a_{II} & a_{IM} \\ a_{MI} & a_{MM} \end{pmatrix} = \begin{pmatrix} s_0 m f_1 + s_I(1 - m) & s_0 f_2 \\ s_M m & s_M \end{pmatrix} \quad (1)$$

, where  $a_{ij}$ , the transition rate, describes the contribution of stage  $j$  individuals to stage  $i$  the next year. With given initial conditions we can compute the number of individuals in the two stages by iterating matrix multiplication by  $A$ .

We implemented density-dependence in this population, so that the population would not continuously increase (see Figure 1). We assumed seed germination and survival parameter  $s_0$  declined with increasing density of mature and immature competitors using a Beverton-Holt function to avoid chaotic behaviors (Caswell, 2001):

$$s_0 = \frac{s_{0,max}}{1 + k_I N_I + k_M N_M} \quad (2)$$

with  $k_I$  and  $k_M$  the weights of immature ( $N_I$ ) and mature ( $N_M$ ) population respectively.  $s_{0,max}$  is the maximum achievable  $s_0$ .

### Phenotype and life-history traits

In this population we observed a single phenotype  $z$ : the bud-burst date. Here, bud-burst date is expressed in julian days (numbered days in the year, 1st of January being 1 in julian days). In our model, an individual is born with a given phenotype and keeps it throughout his life.

We supposed certain life-history traits for each individual -  $s_I$  immature survival,  $f_1$  first reproducers fecundity and  $f_2$  experienced reproducers - (see Equation 1) to be Gaussian function of phenotype  $z$ . Thus, bud-burst date directly influence their values. They can be expressed as follow:

$$\begin{cases} s_I(z) = s_I(\theta_s) \exp\left(-\frac{(z - \theta_s)^2}{2\omega_s}\right) \\ f_1(z) = f_1(\theta_f) \exp\left(-\frac{(z - \theta_f)^2}{2\omega_f}\right) \\ f_2(z) = f_2(\theta_f) \exp\left(-\frac{(z - \theta_f)^2}{2\omega_f}\right) \end{cases} \quad (3)$$

,  $\theta_s$  is the optimal bud-burst date for survival, i.e. phenotype where  $s_I$  is at its maximum  $s_I(\theta_s)$ ;  $\omega_s$  is the width of the Gaussian function, its inversely related to selection intensity: with small  $\omega_s$  values, only a restricted range of bud-burst dates would have important survival rates.  $f_1$  and  $f_2$  have similar expressions, but the optimal bud-burst date  $\theta_f$  is different from  $\theta_s$ ,  $f_1$  and  $f_2$  only differ by their maximum values  $f_i(\theta_f)$ , with  $f_1$  lower than  $f_2$  (see Table 1 to have standard parameters values).

The optimal trait values  $\theta_s$  and  $\theta_f$  differ between stages and life-history components, but trait value does not change along the life of an individual, then there is a trade-off between the two fitness components. And the evolution of the trait affects the life-history of the individual.

If we want to compute mean transition rate  $\overline{a_{ij}}$ , we need to average  $s_I$ ,  $f_1$  and  $f_2$  (ex:  $\overline{a_{IM}} = s_0 \overline{f_2}$ ):

$$E[s_I] = \overline{s_I} = \int p_I(z) s_I(z) dz \quad (4)$$

, with  $p_I(z)$  the distribution of  $z$  in the immature stage, as we study a quantitative trait we suppose  $p_I$  has a Gaussian distribution with mean  $\overline{z_I}$  and width  $P_I$  the phenotypic variance in the immature stage (Lande, 1982). We end with the following expression for  $\overline{s_I}$ :

$$\overline{s_I}(\overline{z_I}) = s_I(\theta_s) \sqrt{\frac{\omega_s}{\omega_s + P_I}} \exp\left(-\frac{(\overline{z_I} - \theta_s)^2}{2(\omega_s + P_I)}\right) \quad (5)$$

We obtain similar expressions for  $\overline{f_1}$  and  $\overline{f_2}$ .

## Iterations at each time step

Assuming the phenotype has a Gaussian distribution, the mean genotypic value of matures and immatures at the next time step is given by (Barfield et al. 2011 Eq.5) :

$$\overline{g_I}' = (c_{IM}\overline{g_M} + c_{II}\overline{g_I}) + (c_{IM}G_M\beta_{a_{IM}} + c_{II}G_I\beta_{a_{II}}) \quad (6a)$$

$$\overline{g_M}' = (c_{MI}\overline{g_I} + c_{MM}\overline{g_M}) + (c_{MI}G_I\beta_{a_{MI}} + c_{MM}G_M\beta_{a_{MM}}) \quad (6b)$$

with  $c_{ij} = \frac{n_j \overline{a_{ij}}}{n_i'}$ , the contribution of stage  $j$  individuals to next years pool of stage  $i$  individuals, as a fraction of  $i$  individuals at the next time step  $n_i'$ ; and  $\beta_{a_{ij}}$  the selection gradient as  $\beta_{a_{ij}} = \frac{\partial \ln \overline{a_{ij}}}{\partial \overline{z}}$  (Barfield et al., 2011). The selection gradient represent the force of directional selection (Lande, 1982).

The first term is a weighted average of mean genotypes contributing to this stage; while the second shows the effect of selection.

To have the formal expressions of  $\beta_{a_{ij}}$  we need to compute the selection gradients on life-history components:

$$\begin{aligned}
\beta_{\overline{s_I}} &= \frac{\partial \ln \overline{s_I}}{\partial \overline{z_I}} = \frac{\theta_s - \overline{z_I}}{\omega_s + P_I} \\
\beta_{\overline{f_1}} &= \frac{\partial \ln \overline{f_1}}{\partial \overline{z_I}} = \frac{\theta_f - \overline{z_I}}{\omega_f + P_I} \\
\beta_{\overline{f_2}} &= \frac{\partial \ln \overline{f_2}}{\partial \overline{z_M}} = \frac{\theta_f - \overline{z_M}}{\omega_f + P_M}
\end{aligned} \tag{7}$$

And because we have for example  $\overline{a_{II}} = s_0 m \overline{f_1} + \overline{s_I}(1 - m)$  we get the selection gradient:

$$\beta_{a_{II}} = \frac{s_0 m \overline{f_1} \beta_{\overline{f_1}} + \overline{s_I} \beta_{\overline{s_I}} (1 - m)}{\overline{a_{II}}} \tag{8}$$

We have a similar recursion for phenotypes (Barfield et al., 2011). They depend on terms of direct transition of individuals from one stage to the other  $\overline{t_{ij}}$  and events leadings to new individuals  $\overline{f_{ij}}$  (and we have  $\overline{a_{ij}} = \overline{t_{ij}} + \overline{f_{ij}}$ ):

$$\overline{z'_I} = c_{II}^t(\overline{z_I} + P_I \beta_{t_{II}}) + c_{II}^f(\overline{g_I} + G_I \beta_{f_{II}}) + c_{IM}^f(\overline{g_M} + G_M \beta_{f_{IM}}) \tag{9a}$$

$$\overline{z'_M} = c_{MI}^t(\overline{z_I} + P_I + \beta_{t_{MI}}) + c_{MM}^t(\overline{z_M} + P_M + \beta_{t_{MM}}) \tag{9b}$$

, with  $\beta_{t_{II}}$  the gradient of selection defined as above in Equation 6a, i.e.  $\beta_{t_{II}} = \frac{\partial \ln \overline{t_{II}}}{\partial \overline{z_I}}$ ;  $c_{ij}^t = \frac{n_j \overline{t_{ij}}}{n'_i}$  the contribution by direct transition of stage  $j$  to stage  $i$  and  $c_{ij}^f = \frac{n_j \overline{f_{ij}}}{n'_i}$  the contribution by birth.

## Approximation under weak selection

Under weak selection, the mean phenotype at equilibrium in the population  $\overline{z}$  follows in constant environment (Engen et al., 2011):

$$\overline{z_{eq}} = \frac{\gamma_f \theta_f + \gamma_s \theta_s}{\gamma_f + \gamma_s} \tag{10}$$

, with,

$$\gamma_f = \frac{v_I u_I s_0 m \overline{f_1}}{\lambda(P_I + \omega_f)} + \frac{v_I u_M \frac{G_M}{G_I} s_0 \overline{f_2}}{\lambda(P_M + \omega_f)} \tag{11a}$$

and

$$\gamma_s = \frac{v_I u_I \overline{s_I} (1 - m)}{\lambda(P_I + \omega_s)} \tag{11b}$$

$\gamma_f$  and  $\gamma_s$  represent the respective weight of each of the optimum in the trade-off between  $\theta_f$  and  $\theta_s$  for  $\overline{z_{eq}}$ . Indeed, if  $\theta_f = \theta_s$  then  $\overline{z_{eq}} = \theta_f = \theta_s$ . But if  $\theta_f \neq \theta_s$ , then the mean phenotype on the trade-off depends on  $\gamma_f$  and  $\gamma_s$  and the ratio between them.

## Fluctuating optimums

During my internship, I tried to mimic environmental fluctuations, by making the optima fluctuate as such:

$$\begin{cases} \theta_f(t) = \overline{\theta_f} + \alpha_f \xi_f \\ \theta_s(t) = \overline{\theta_s} + \alpha_s \xi_s \end{cases} \tag{12}$$

$\alpha_i$  is the sensitivity of  $\theta_i$  to noise  $\xi_i$ .  $\xi_f$  and  $\xi_s$  are noise vectors drawn at each time step from a bi-variate normal distribution with respectively  $\sigma_f^2$  and  $\sigma_s^2$  variances and correlation  $\rho_N$ . Thus we get normal fluctuations, correlated with a correlation coefficient of  $\rho_N$ .

Under varying environment we get another approximation under weak selection from (Engen et al., 2011) describing the change of mean phenotype:

$$\Delta \bar{z}(t) = -G_I \gamma (\bar{z}(t) - \theta_v(t)) \quad (13)$$

, with

$$\gamma = \gamma_f + \gamma_s \quad (14a)$$

$$\theta_v(t) = \bar{z}_{eq} + \xi_v \quad (14b)$$

$$\xi_v = \frac{\alpha_f \xi_f + \alpha_s \xi_s}{\alpha_f + \alpha_s} \quad (14c)$$

We see that the change in the mean phenotype depends on the sensitivity of the optima  $\alpha_i$  as well as on the magnitude of the variations.

## Trend in change

To model climate-change, and especially the trend to increase temperature with time, we included a trend in the variation of the optima. The optima still experience fluctuations as above they linearly vary with time:

$$\begin{cases} \theta_i(t) = \bar{\theta}_i + \alpha_i \epsilon(t) \\ \epsilon(t) = kt + \xi_i \end{cases} \quad (15)$$

With  $k$  having a negative value, the optima decrease with time.

## PHENOFIT data

PHENOFIT is a phenology model including several sub-models, from environmental and phenological data it simulates the survival and reproduction of an average tree to predict its range (Morin et al., 2008).

We used output from PHENOFIT (simulations performed by A. Duputié) from 1950 to 2100 for the sessile oak (*Quercus petraea*) about predicted bud burst date and predicted fitnesses in 6 localities (see Figure 4). We had fitness predictions for phenotype around the modeled date (a range of 21 days). From these data we predicted the optima fluctuations. Considering fecundity  $f$  as a Gaussian function around this date with the same form as  $f_1$  in Equation 5:

$$\beta = \frac{\partial \ln f}{\partial \bar{z}} = \frac{\theta_f - \bar{z}}{\omega_f + \sigma_z^2} \quad (16)$$

Using (Lande and Arnold, 1983), with  $z$  Gaussian,  $p(z)$  the distribution of  $z$  in the population,  $f(z)$  the fitness associated with  $z$  and  $\bar{f}$  the mean fitness in the population, we computed selection gradients from PHENOFIT simulation outputs as::

$$\beta = \frac{\text{cov}(z, \frac{f(z)}{\bar{z}})}{\sigma_z^2} \quad (17)$$

From (16) and (17) we can express  $\theta_f$ :

$$\theta_f = \frac{\text{cov}(z, \frac{f(z)}{\bar{z}})}{\sigma_z^2} (\omega_f + \sigma_z^2) + \bar{z} \quad (18)$$

In our estimations we considered  $p(z)$  to be Gaussian around the modeled date by PHENOFIT, with a variance of  $P_I = 40$  as in our analytic model. We normalized this distribution so that all dates in the population would be in the 42 days interval around the modeled date.

## Trend analyses

All statistical analyses were made using R (R Core Team, 2014), graphics were drawn using ggplot2 (Wickham, 2009), data were handled using dplyr (Wickham and Francois, 2014).

To estimate the trend of the  $\theta_f$  variations, we considered a trend model with three components: a general decreasing linear trend, a white noise component with a constant variance and a more dramatic noise leading to "catastrophic" events, with negative  $\theta_f$  values.

The regular noise and the trend were estimated excluding those catastrophic events, we kept only value of  $\theta_f$  over 60, which is the lower bound of the realizable range of bud burst date of oak trees. Then we performed a linear regression between values of  $\theta_f$  and time, giving us an estimation of  $k$  from Equation 15. Analyzing the residuals gives us the variance of  $\alpha_f \xi_f$  from the same equation.

## Results

### Constant environment and density-dependence

We used the previously developed model in (Sandell et al. 2014, master's thesis) and simulated (see Figure 1) a tree population for 150 years in a constant environment, with and without density-dependence on  $s_0$ , assess the effects of a more realistic demography.

As expected, density-dependence allow regulating the population (Figure 1 right panel), as the number of mature and immature individuals seem to converge respectively to 18000 and 10000 individuals, while without density-dependence the population is exponentially growing.

Looking at the phenotype, we started from exactly the same starting point  $z = 116$  for phenotypic and genotypic values. Without density-dependence, the population quickly converge to the equilibrium phenotype ( $\overline{z_{weak}}$  given by the approximation in Equation 10),  $\overline{z_{weak}} = 116$  in this case. With density-dependence the equilibrium is shifted towards the survival optimum  $\theta_s$  ( $\overline{z_{weak,dd}} = 121.8$ ,  $\theta_s = 130$  while  $\theta_f = 100$ ).

The lower seed survival  $s_0$  decreases  $\gamma_f$  (11a) changing the weights in (10), making it more interesting to favor the survival of already established immature trees than the production of many propagules with very little survival prospect.

The genotypic values,  $\overline{g_I}$  and  $\overline{g_M}$  (respectively gray and black on Figure 1) are clearly distinct from the mean phenotype values.

Within the density-dependent model the mean immature phenotype  $\overline{z_I}$  converge quicker than the mean mature phenotype  $\overline{z_M}$  to the equilibrium. It is because of stage-structured nature of our model, the mature stage is a combination of individuals that lived for around 40 generations (given our life-cycle), it buffers adaptation. To make  $\overline{z_M}$  closer to  $\overline{z_{weak}}$ , immature individuals with a phenotype closer to  $\overline{z_{weak}}$  need to survive long enough to mature and outnumber initial mature individuals with phenotype further from  $\overline{z_{weak}}$ .

### Fluctuating optima

To mimic a changing environment we made the optima fluctuate (Figure 2, dashed lines) and compared this model to the one in constant environment (solid lines).

The mean phenotype of the population does not change very much with the fluctuations, indeed,  $\overline{z_M}$  in constant and fluctuating environment are equal, and they are also equal to  $\overline{z_{eq}}$ , that is why they are indistinguishable on Figure 2.

Only  $\overline{z_I}$  fluctuates under varying environment, but the fluctuations have a very small variance compared to the ones of the optima. We found a good correlation between fluctuating  $\theta_s$  and  $\overline{z_I}$  ( $\rho_{\text{Pearson}} = 0.6997364$ ), no other correlation between  $\theta_f$  or  $\overline{z_M}$  are as high as this one. It shows how

Parameter	Notation	Value
<b>Life Cycle</b>		
Optimal phenotype for fecundity	$\theta_f$	100
Optimal phenotype for immature survival	$\theta_s$	130
Fecundity function width	$\omega_f$	400
Survival function width	$\omega_s$	400
Heritability	$h^2$	0.5
Phenotypic variance of immatures	$P_I$	40
Phenotypic variance of matures	$P_M$	40
Genotypic variance of immatures	$G_I = P_I \times h^2$	20
Genotypic variance of matures	$G_M$	20
Survival of immature at phenotypic optimum	$\overline{s_I}(\overline{z} = \theta_s)$	0.8
Fecundity of first time reproducers at optimum	$\overline{f_1}(\overline{z} = \theta_f)$	100
Fecundity of experienced reproducers at optimum	$\overline{f_2}(\overline{z} = \theta_f)$	200
Maturation rate of immature	$m$	0.02
Combined survival and germination rate of seed	$s_0$	0.03
Survival of mature stage	$s_M$	0.99
<b>Density-dependence</b>		
Maximum $s_0$ in density-dependence function	$s_{0,max}$	0.12
Decreasing factor due to immatures	$k_I$	0.001
Decreasing factor due to matures	$k_M$	0.005
<b>Fluctuations</b>		
Sensitivity of optimum for fecundity to fluctuation	$\alpha_f$	5
Sensitivity of optimum for survival to fluctuation	$\alpha_s$	5
Noise variance for fecundity	$\sigma_{\xi_f}^2$	3.725
Noise variance for survival	$\sigma_{\xi_s}^2$	3.725
Correlation between noises	$\rho_N$	0.5
Trend coefficient	$k$	-0.15

**Table 1:** Standard parameter set

immature individuals track very smoothly the variations of the survival optimum and invest specifically more on this one.

Because of the variations, the mean of  $s_I$  in fluctuating environment is lower than in constant environment, it explains why the number of immature individuals  $N_I$  is lower under the fluctuating regime thus decreasing the number of mature individuals  $N_M$ , in the end it increases  $s_0$  by density-dependence. The variation in  $\theta_s$  causes  $s_I$  to decrease, it underlines the cost of the fluctuations demographically: fluctuating regime causes variations in survival that may have dramatic effect on population.

However, those fluctuations do not seem to affect fecundities  $f_1$  and  $f_2$  in the same way (Figure 2 bottom left panel). As the mean optima move they get closer to population phenotype increasing fecundity, but the next time step they move further away from this phenotype and they decrease fecundity.

The asymmetry of responses between, from the one hand,  $s_I$ , and from the other hand,  $f_1$  and  $f_2$ , can be explained by the specific trade-off occurring in our population. The mean phenotype in our simulations is closer to  $\theta_s$  than to  $\theta_f$ , there is a higher chance of  $\theta_s$  to be lower or much higher than the mean population phenotype, then there is for  $\theta_f$  to cross the mean population phenotype line.

As we had partially correlated noises in our population (see Table 1 to have standard parameters set), we vary correlations for noises between 0 and 1. The results were consistent whatever the correlation coefficient. It seemed that the lower the correlation between noises, the higher were the demographic burden. Uncorrelated environments decrease more the life-history traits than correlated environments.

## Trend in the environment

We implemented a decreasing trend in  $\theta_f$  with fluctuations (Figure 3) to mimic climate change. We simulated both a linear trend and a linear trend with fluctuations in optima variation (respectively solid and dashed lines in Figure 3).

The phenotype in the population decreases as the optima decrease, but much slower, whether with fluctuations or not. The mean phenotype in the immature stage  $\bar{z}_I$  seem to vary in the same fashion with and without fluctuations, while the mean phenotypes among mature individuals  $\bar{z}_M$  are almost indistinguishable in the two environments,  $\bar{z}_M$  under fluctuations (dashed line) is a little bit over  $\bar{z}_M$  without them (solid line). We implemented the approximation  $\bar{z}_e$  from (Engen et al., 2011), it seems to follow the variations in a similar fashion as the mean phenotype in the population.

$s_I$  has an interesting behavior, it first increases, reaches a maximum, then decreases. The decreasing trend in optima variation causes at first the mean population phenotype to move closer to  $\theta_s$ , thus maximizing  $s_I$  values when it crosses  $\theta_s$  line, as soon as it moves beyond  $s_I$  starts to decrease again. The fluctuations seem to decrease  $s_I$  (mean difference of 0.5), it may be a cost associated with the variance of optimum fluctuations, the optimum is often under the mean population value.

On the contrary  $f_1$  and  $f_2$  do not show a different pattern with or without fluctuations. They decrease because the mean population phenotype go further away from  $\theta_f$ .

Seed germination and survival  $s_0$  is increased by fluctuations, via an indirect mechanism: fluctuations decrease immature survival  $s_I$ , thus decreasing the immature population  $N_I$  and so the mature population  $N_M$ ; this population decrease also decrease competition and density, increasing  $s_0$  as it is density-dependent (see Equation 2).

As expected, the decreasing trend in  $\theta_f$  creates a lag between the optima and the mean population values, because adaptation is slower than the rate of change. However, the population can still survive with such a rate if the difference between the optima and the means become constant. On a very long scale (2500 years) it is what happens in this case, the population maintain by changing its phenotype fast enough to track the optima variation (data not shown).



## Estimation of the fluctuations

In 6 localities (map [Figure 4](#) bottom left) using PHENOFIT output, we computed  $\theta_f$  values at these locations (top 3 rows of [Figure 4](#)). For the 6 sites, predicted  $\theta_f$  decrease with time, it is more precocious as time passes. This observation matches the advance of phenology observed in the literature because of climate change.

Over the general trend, we observe a small amplitude variation (with a standard deviation of 9.6 d), corresponding to year to year change in  $\theta_f$  and some dramatic decreases in its values, sometimes reaching negative values (For example at BIC site in 1976). The frequency of these events increase with time as they become common after 2050 for all sites. Note that those events are biased towards the decrease of  $\theta_f$ , as there is no equivalent dramatic increases.

The negative values of  $\theta_f$  computed in [Figure 4](#), may seem striking as there is no such thing as a negative bud-burst date! It indicates strong directional selection to shorten bud-burst those years with very little sign of quadratic selection on that trait. As bottom right panel of [Figure 4](#) shows, we can have negative value of  $\theta_f$  and still have achievable phenotypes. If  $\theta_f$  is very negative for a given year (less than -100 in 2048 for LAB), it means there will be no reproduction this year (flat tail of blue curve, bottom right oanel [Figure 4](#)).

We excluded those extreme events, taking all sites together, to estimate the trend in the variation of  $\theta_f$  (see [Materials and Methods](#)). Using linear regression on  $\theta_f$  with time, we found a rate of  $-0.15 \text{ d yr}^{-1}$ , with normal residuals having a variance of  $105 \text{ d}^2$  (data not shown,  $R^2 = 0.2341$ ,  $p < 2\text{e-}16$ ,  $F = 186.7$  with 611 d.f.).

We investigated whether there was a break between years modeled from real data by PHENOFIT (before 2001) and years modeled using climate models with climate change included (from 2001). We performed the same regression as above ( $\theta_f$  with time), without taking apart the extreme values, for all sites, splitting the data before 2001 and after 2001 (data not shown). For each site, the slope estimates were non-significantly different from zero for years before 2001, while we had very steep slopes estimates after 2001 between  $-0.7 \text{ d yr}^{-1}$  and  $-1.1 \text{ d yr}^{-1}$ .

## Discussion

We modeled a stage-structured tree population using a quantitative genetics approach, with bud-burst date the studied trait varying between two optima. We used it to understand their phenotype evolution in the next 150 years. Using PHENOFIT simulation results we computed values for one of the optima. An increasing number of extreme events would happen in the next century.

As expected in the literature, we found a decreasing trend in the variation of optima, i.e. a trend to precocity of phenology ([Aitken et al., 2008](#); [Ehrlén and Münzbergová, 2009](#)). Because of the general increase in temperature, organisms advance their phenology to track their original environment.

Long-lived stage structure populations don't have show strong reaction to fluctuations nor to climate change -> beware of the "buffer" effect, due to life cycle

Fluctuations don't have strong effect on phenotype but on demography

Increasing number of catastrophic events

Our model -> need more realistic variations including "catastrophic events", include phenotypic plasticity, understand better the difference between breeding values and phenotypes, predict extinction time?

## References

Aitken, S. N., Yeaman, S., Holliday, J. A., Wang, T. and Curtis-McLane, S. (2008). Adaptation, migration or extirpation: climate change outcomes for tree populations. *Evolutionary Applications*



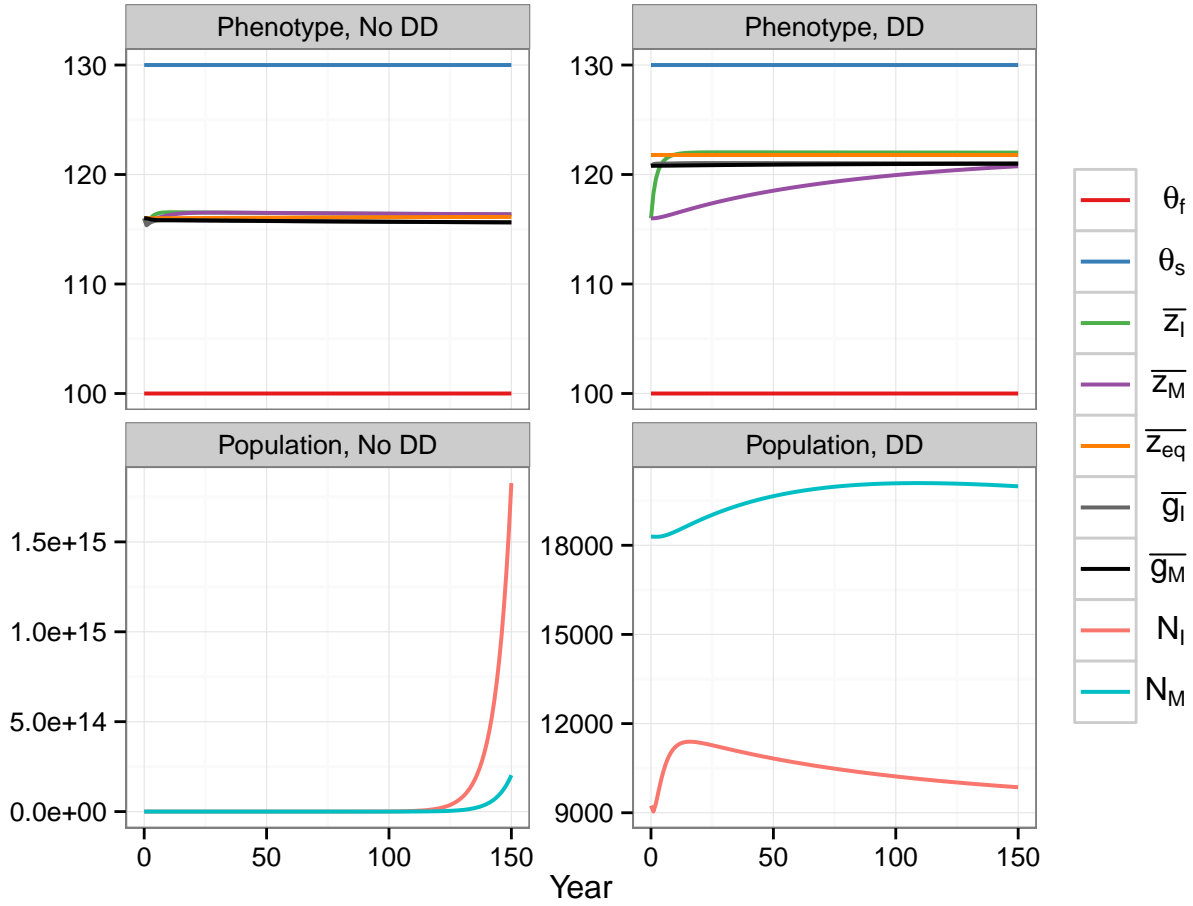


**Figure 1: Effect of density-dependence on phenotypes and populations.** **Top:** Phenotype variations in population ( $\bar{z}_I$ ,  $\bar{z}_M$ , starting from  $z = 116$ ) with their corresponding genotypic values ( $\bar{g}_I$ ,  $\bar{g}_M$ ), and the approximation given by Equation 10; **Bottom:** Population, number of immature individuals ( $N_I$ , red), number of mature individuals ( $N_M$ , blue). Starting from Stable-Stage Distribution (SSD) in constant environment. **No DD** means we used the model without density-dependence, **DD** means we implemented density-dependence through  $s_0$  (see Equation 2).

*I*, 95--111.

- Barfield, M., Holt, R. D. and Gomulkiewicz, R. (2011). Evolution in Stage-Structured Populations (2 versions). *The American Naturalist* 177, 397--409.
- Caswell, H. (2001). Matrix population models : construction, analysis, and interpretation. Sinauer Associates.
- Ehrlén, J. and Münzbergová, Z. (2009). Timing of Flowering: Opposed Selection on Different Fitness Components and Trait Covariation. *The American Naturalist* 173, 819--830.
- Engen, S., Lande, R. and Sæther, B.-E. (2011). Evolution of a Plastic Quantitative Trait in an Age-Structured Population in a Fluctuating Environment. *Evolution* 65, 2893--2906.
- Lande, R. (1982). A Quantitative Genetic Theory of Life History Evolution. *Ecology* 63, 607--615.
- Lande, R. and Arnold, S. J. (1983). The Measurement of Selection on Correlated Characters. *Evolution* 37, 1210--1226.

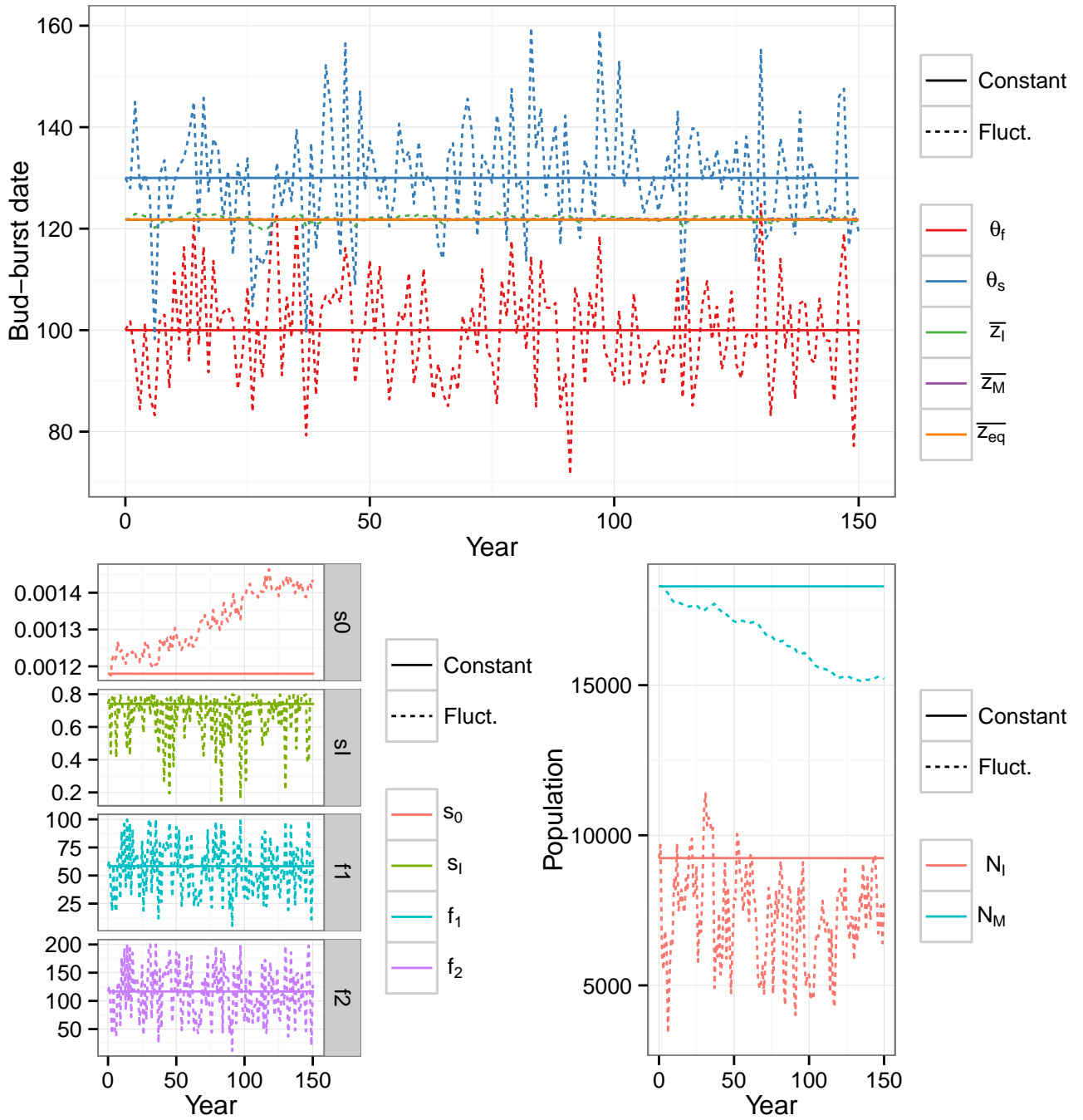


**Figure 2: Fluctuating optima against constant environment.** **Top:** comparison of phenotypes from simulations with constant or fluctuating optima,  $\bar{z}_{eq}$  is the approximation shown in Equation 10. **Bottom: (Left)** life-history traits in constant or fluctuating environment, **(Right)** population in constant or fluctuating environment,  $N_I$  is the number of immature individuals and  $N_M$  the number of mature individuals, population started from the stable stage distribution. **Solid lines:** values in constant environment, **Dashed lines:** in fluctuating environment.

Morin, X., Viner, D. and Chuine, I. (2008). Tree species range shifts at a continental scale: new predictive insights from a process-based model. *Journal of Ecology* 96, 784--794.

R Core Team (2014). R: A Language and Environment for Statistical Computing. R Foundation for Statistical Computing Vienna, Austria.

Wickham, H. (2009). *ggplot2: elegant graphics for data analysis*. Springer New York.

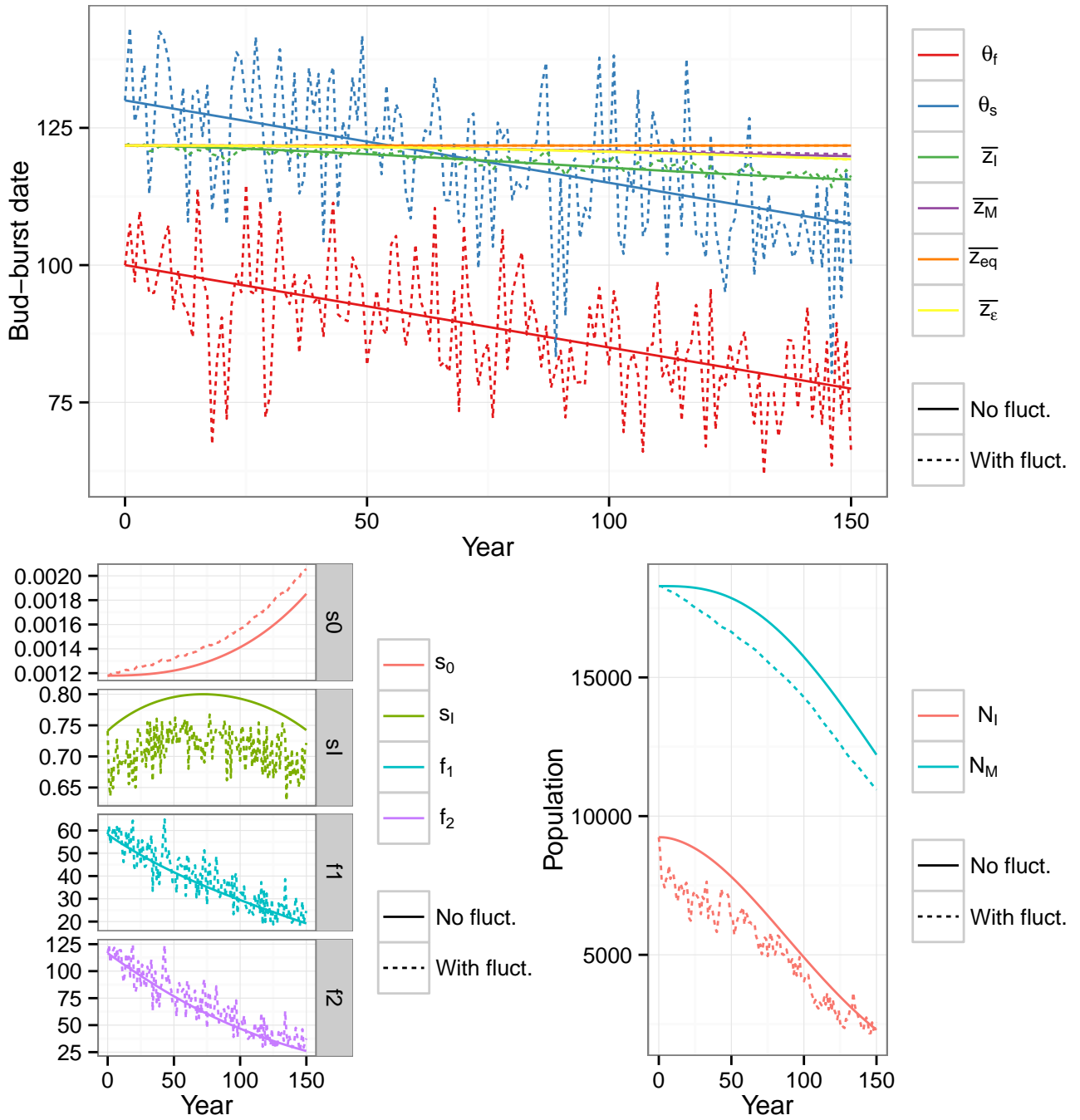


**Figure 3: Mixed influences of trend and fluctuations on the population.** **Top:** Phenotype evolution with and without fluctuations, results from a **single** simulation; **Bottom: (Left)** life-history traits evolution; **(Right)** demography. **Solid lines: (No fluct.)** linearly decreasing optima with time; **Dashed lines: With fluct.** fluctuating decreasing optima. Life-history traits and population were averaged over 15 independent population to buffer the stochasticity of simulations.

Wickham, H. and Francois, R. (2014). dplyr: A Grammar of Data Manipulation. R package version 0.3.0.2.

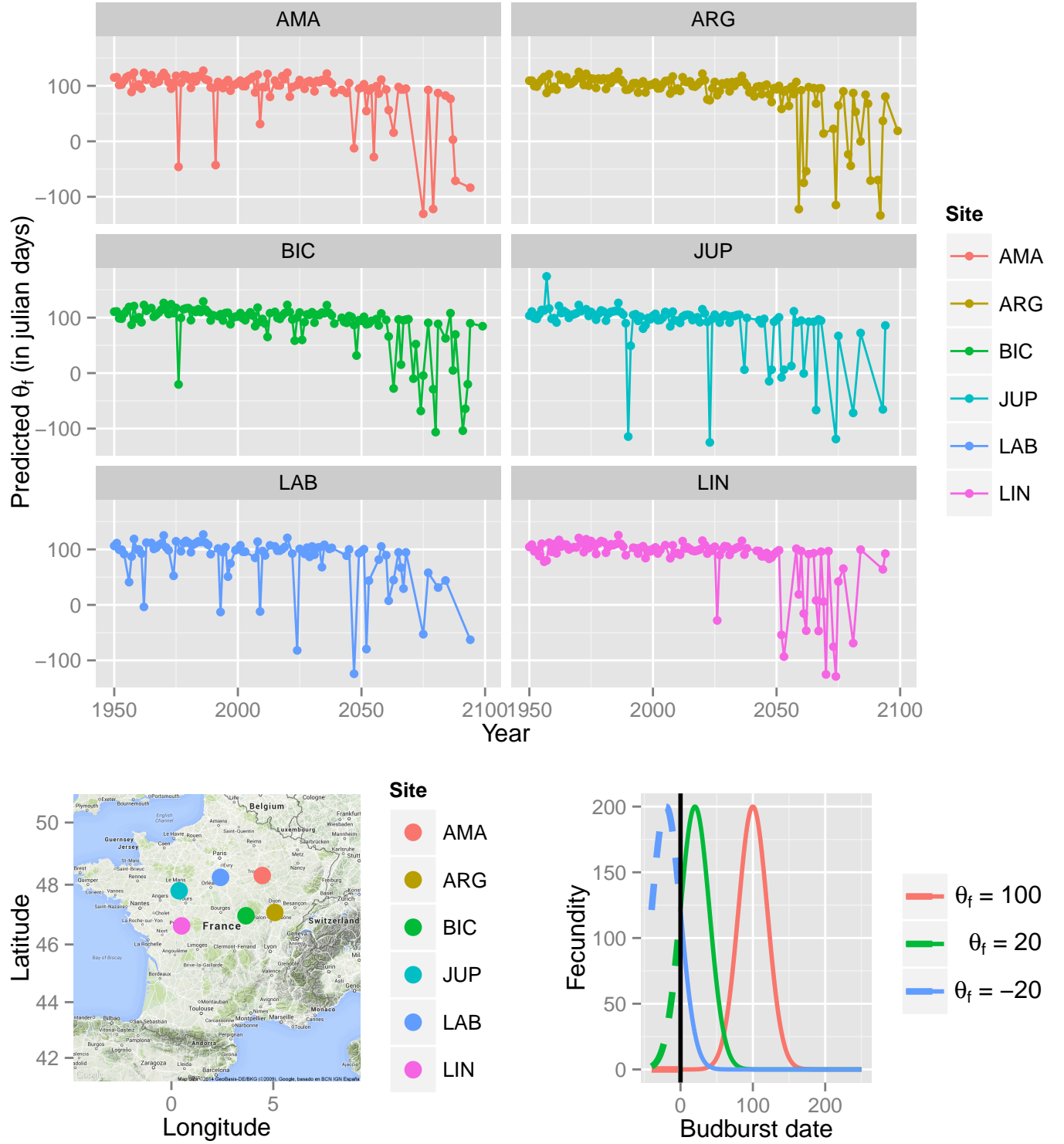


**Figure 4:**  $\theta_f$  estimations from PHENOFIT data. **Top:** estimations of  $\theta_f$  for each study site (see [Materials and Methods](#) for details). **Bottom: (Left)** map of the study sites; **(Right)** Theoretical fecundity functions with parameters from [Table 1](#) with values of  $\theta_f$  equals to 100, 20 and  $-20$ , solid lines indicate achievable phenotype, dashed lines show theoretical curves but unreachable phenotypes.